Odontology (2021) 109:53–66
https://doi.org/10.1007/s10266-020-00529-5

ORIGINAL ARTICLE

Effects of a derivative of reutericin 6 and gassericin A on the biofilm of *Streptococcus mutans* in vitro and caries prevention in vivo

Jingheng Liang[1] · Dongsheng Liang[2] · Yuee Liang[1] · Jianing He[1] · Shiya Zuo[1] · Wanghong Zhao[1]

Received: 6 January 2020 / Accepted: 18 May 2020 / Published online: 30 May 2020

Abstract

It is known that *Streptococcus mutans* (*S. mutans*) is the leading cariogenic pathogen. Recently, an increasing number of antimicrobial peptides (AMPs) have been brought into consideration as anti-caries agents. Here, we designed and synthesized an AMP derived from reutericin 6 and/or gassericin A, named **LN-7**, and explored its effect on biofilm of *S. mutans* UA159 in vitro and development of dental caries in vivo. Antibacterial assays showed that **LN-7** was more active against *S. mutans* (3.2 μM) than many peptide-based agents, capable of killing other types of Streptococci in oral cavity. In addition, **LN-7** presented fast killing kinetics, with more than 97% *S. mutans* killed within 5 min. The mechanism of the antimicrobial activity mainly lies on the disruption of bacterial membrane. Effects of **LN-7** on the biofilm formation and the viability of preformed biofilm were quantified by crystal violet staining, which showed that **LN-7** could effectively inhibit the biofilm accumulation of *S. mutans*. Moreover, the biofilm of *S. mutans* treated with **LN-7** displayed notable changes in bacterial viability and morphology, observed by confocal laser scanning microscopy and scanning electron microscopy. In addition, topical oral treatment with **LN-7** could suppress the development of dental caries in vivo, reducing the occurrence of severe dental lesion in a rodent model. These results reveal a new peptide-based agent as a topical treatment for dental caries, opening the door to clinical studies to explore its potential for caries prevention.

Keywords Dental caries · Antimicrobial · Biofilm · *Streptococcus mutans* · Peptide

Introduction

Dental caries is a prevalent chronic microbially mediated human disease worldwide, increasing global economic burden and causing common health concerns. Without appropriate prevention or treatment, it will eventually cause toothache pain and tooth loss, or even develop into maxillofacial infection. It is widely accepted that dental caries is primarily caused by the biofilm communities attached to the surface of the teeth, known as dental plaque [1].

Dental plaque is a complex biofilm system, consisting of a collection of microbial communities enclosed by a matrix of extracellular polymeric substance (EPS) and separated by a network of open water channel [2]. This kind of biofilm system is the prime cause for not only dental caries, but also other oral diseases, such as halitosis, peri-implantitis, periodontitis, and so on [3, 4]. Studies have shown that the regions of the oral cavity could harbor and create different micro-environments with the selection of several species [5]. For instance, in the sample of the tongue dorsum biofilm from halitosis-suffering patients, it was found that *Streptococcus* spp. seemed to be the most prevalent as early colonizers and *F. nucleatum* served as a bridge between early and late colonizers within the oral biofilm [2]. On the other hand, *Streptococcus sanguinis* was found to be the microorganism fundamental to the beginning of biofilm formation in patients with peri-implanting mucositis and peri-implantitis [5–7].

Electronic supplementary material The online version of this article (https://doi.org/10.1007/s10266-020-00529-5) contains supplementary material, which is available to authorized users.

✉ Wanghong Zhao
zhaowh@smu.edu.cn

[1] Department of Stomatology, Nanfang Hospital, Southern Medical University, 1838 Guangzhou Avenue North, Guangzhou 510515, People's Republic of China

[2] Department of Stomatology, Affiliated Zhongshan Hospital of Sun Yat-sen University, Guangzhou, People's Republic of China

As for the natural teeth with dental caries, within the biofilm attached to its surface, *Streptococcus mutans* (*S. mutans*) was considered to be the main cariogenic bacteria because of its several cariogenic virulence properties, such as acidogenicity, acidurance, and the ability to interact with other microorganisms to build multispecies biofilm communities [1]. The particular condition of biofilm protects the microbes from environmental damage factors, including host immune cells and drug treatments, and also keeps the microenvironment stable at low pH, resulting in the demineralization of tooth enamel [4, 8]. Therefore, inhibiting the growth of *S. mutans*, blocking the formation of biofilm, and disrupting the preformed biofilm are the main strategies to prevent dental caries [9]. Traditional pharmacy approaches to prevent dental caries mainly include the use of antimicrobial agent, such as chlorhexidine (CHX), erythromycin, and fluoride-containing products [10, 11]. However, it has been proved that these methods could only exhibit a minimal inhibitory effect on biofilm-encased cells [12]. Furthermore, long-term use of chlorhexidine and fluoride-containing products have several adverse effects, including tooth staining, loss of taste perception, and rising incidence of dental and skeletal fluorosis [11, 13].

To address these concerns, more and more research emphasized the potential of antimicrobial peptides (AMPs) as potent alternatives to traditional antimicrobial agents recently. AMPs are short cationic host-defense molecules composed of 3–50 amino acids and play important modulatory roles in the immune system, effective at low micromolar concentrations against a broad range of microorganisms, including drug-resistant strains [14]. A growing body of evidence supports the notion that AMPs play an important part in maintaining the balance between health and disease in the complicated oral environment [15]. Currently, there are roughly 20 AMPs in different developmental phases, from preclinical to clinical phase Ill trials, four of which are applied to oral disease [16]. Moreover, many natural or synthetic AMPs were studied to assess the ability against cariogenic bacteria, such as α- and β-defensin [17], cathelicidin LL-37 [18], pleurocidin [19], chrysophsin-1 [20], histatin 5 [21], and Bac8c [22], yet no AMPs have been applied to clinical treatment for dental caries.

Reutericin 6 and gassericin A, circular bacteriocins produced by oral commensal bacteria *Lactobacillus* species, could inhibit the growth of *S. mutans* and its biofilm formation [23–25]. It is worth noticing that they were proved to be related to lower levels of dental plaque in vivo [24]. The sequences of them are identical (58 common amino acids), but the secondary structures are different [26]. However, because of their long circular structure, the synthesis of them is complicated and high-costing.

The objectives of this study were (1) to design and synthesize a novel short linear reutericin 6 and/or gassericin A-inspired peptide, (2) to subsequently demonstrate its activity against planktonic cultures and biofilms of *S. mutans* in vitro, also its killing kinetics and modes of action, and (3) to further explore its effect on the prevention of dental caries in vivo. Worth mentioning, to the best of our knowledge, this work is the first to observe anti-caries effects of a peptide derived from reutericin 6 and gassericin A in a rodent model of dental caries in vivo.

Materials and methods

Peptide design and synthesis

First, from the cationic α-helical region of reutericin 6 and/or gassericin A, a 13-residue linear peptide was truncated and named as LR-1. Then, the subsequent modification was based on the principle of amphipathicity and cationicity. Arginine residues were chosen to substitute the non-polar and negatively charged residues on the polar faces of LR-1 to increase its cationicity. Meanwhile, tryptophan and lysine residues were used to substitute the non-hydrophobic residues on the non-polar face to enhance the AMP's antimicrobial activity [27–29]. Eventually, an AMP with increasing cationicity and hydrophobicity was obtained and named **LN-7**, with a sequence of LRRWLRWLLRWMR-NH_2. The peptide was synthesized using standard 9-fluorenylmethoxycarbonyl (Fmoc) solid-phase protocols on Rink Amide MHBA resin (Nanjing Peptide Biotech Ltd, Nanjing, China). The C-terminal of the peptides was amidated to remove a negative charge at neutral pH. It was purified to >95% by RT-HPLC and their molecular weights were measured by mass spectrometry. Prior to assessing antimicrobial activities, the peptide was dissolved in sterile deionized water at a concentration of 5 mg/mL and stored at − 20 °C.

Strains and growth condition

Streptococcus mutans UA159 (*S. mutans* UA159), *S. mutans* ATCC25175 (*S. mutans* ATCC25175), *Streptococcus gordonii* ATCC10558 (*S. gordonii* ATCC10558), *Streptococcus sobrinus* ATCC33478 (*S. sobrinus* ATCC33478), and *Enterococcus faecalis* ATCC29212 *(E. faecalis* ATCC29212) were acquired from the Guangdong Microbial Culture Collection Centre (GDMCC; Guangdong, China). Brain–heart infusion (BHI) broth was used for anaerobic culture (10% CO_2, 10% H_2, 80% N_2) at 37 °C.

Bacterial susceptibility assay

Minimal inhibitory concentrations (MIC) and minimum bactericidal concentrations (MBC) were measured by the standard broth microdilution method following the

recommendations of the Clinical and Laboratory Standards Institute (CLSI) with some modifications [30]. Bacterial strains grown overnight at 37 °C were diluted to a final concentration of 1.0×10^6 CFU/mL and treated with **LN-7**, erythromycin (Sangon Biotech, Shanghai, China), or CHX (Sangon Biotech, Shanghai, China). The final test concentration for **LN-7** ranged from 0.4 to 51.2 μM. Erythromycin and CHX were used as the positive controls ranging from 0.03 to 32.0 μM. Medium without bacteria served as the negative control. The experiments were performed in 96-well microtiter plates. The plates were incubated anaerobically at 37 °C for 1–2 days. MICs were determined as the lowest concentration of drugs that inhibited bacterial growth by visual inspection after 24 h of incubation. MBCs were defined as the lowest concentration resulting in no bacterial growth after 48 h of incubation with bacterial suspension spread on BHI.

Time-killing assay

The killing kinetics of the **LN-7** against *S. mutans* UA159 were analyzed using a time-killing assay as previously described [31–33]. In brief, *S. mutans* was diluted to 1.0×10^6 CFU/mL in the BHI medium. Solutions of **LN-7** at final concentrations of 6.4 and 12.8 μM (1× MBC and 2× MBC) were added to the bacterial suspension, with 19.8 μM (2× MBC) chlorhexidine and 2.7 μM (2× MBC) erythromycin as positive controls, and a non-treated group as the negative control. The cell survival was estimated by colony enumeration on BHI agar after treatment at 37 °C for 0, 0.5, 1, 1.5, 3, 5, 7, 9, 10, 15 and 30 min. The percent survival was determined by dividing the viable cell CFU/ml by the total CFU/ml in the untreated controls.

To further investigate the killing kinetics of the **LN-7**, optical density assays were performed as follows: *S. mutans* UA159 were cultured overnight, centrifuged at 1000 *g* for 10 min, and diluted to 1.0×10^6 CFU/ml with PBS after harvest. **LN-7** at final concentrations of 6.4 and 12.8 μM was then added to the bacterial suspension for 0, 5, 15, 30, 60, 90, and 120 min at 37 °C. 3.5 μM melittin was used as a positive control. A non-treated group was used as a negative control. The mixture was filtered through a filter membrane (0.22 μm), and the optical density at 260 nm of the filtrates was measured by ultraviolet spectrophotometer (UV757CRT, Lengguang Tech., China).

In addition, to determine the antimicrobial effects of **LN-7** on other types of Streptococci in oral cavity (*S. sobrinus* ATCC33478 and *S. gordonii* ATCC10558) at a cell density of 1×10^6 CFU/ml, bactericidal kinetics was also examined as described above, but only upon treatment with solution of **LN-7** at final concentrations of 1 × MBC.

Biofilm susceptibility assays

Inhibition of *S. mutans* biofilm formation was examined using the crystal violet-based microtiter plate assay described originally by O'Toole and Kolter [34]. *S. mutans* UA159 was grown in BHI broth with 1% (w/v) sucrose (BHIS) and diluted to a final concentration of 1.0×10^6 CFU/mL, treated with **LN-7**, chlorhexidine, or erythromycin. The concentrations tested were 0.6×, 0.8×, 1×, 2×, 4× and 8× their respective MICs. After incubation at 37 °C for 24 h, the supernatant medium was removed, and all wells were washed three times with PBS. And then, 100 μL of methanol was added to fix adhered cells for 15 min. After the removal of methanol, 100 μL of 0.1% crystal violet was added for 5 min to stain adhered biomass. Excess dye was removed and rinsed with water, then the wells were air-dried for 1 h. To quantify the biomass, crystal violet stains were solubilized in 95% ethanol for 30 min and the optical densities were measured at the wavelength of 595 nm using a microplate reader. Biofilm formation was expressed as a ratio of crystal violet-stained biofilms relative to the untreated control. Biofilm was treated with chlorhexidine and erythromycin as positive controls.

Moreover, the antibiofilm activities of **LN-7** were examined against preformed biofilm as described previously with a minor modification [10]. *S. mutans* UA159 was adjusted to 1×10^6 CFU/ml in BHIS and seeded on to 96-well polypropylene flat-bottomed plates. Biofilms were established anaerobically at 37 °C for 24 h. After incubation, non-adherent cells were removed carefully. Biofilms were then treated with **LN-7**, CHX, or erythromycin at final concentrations of 0, 1×, 2×, 4×, 8× and 10× their respective MICs in fresh BHIS for 24 h. To count the viable cells within treated biofilms, plates were sonicated for 5 s to dislodge the adherent bacteria. Then, the bacteria were removed mechanically from biofilms by scraping with pipette tips and rigorous vortex. The bacterial suspension was spread on BHI agar and incubated anaerobically at 37 °C for 2 days before colony enumeration.

Confocal laser scanning microscopy

S. mutans UA159 was cultured in BHIS for 24 h and diluted to a final concentration of 1.0×10^6 CFU/mL and then seeded in 6-well plates with coverslips in each well to establish biofilms. 1-day old *S. mutans* biofilms were treated with **LN-7**, CHX or erythromycin at the concentration of 10× MIC at 37 °C for 24 h. A no-treatment group was used as the negative control. After that, the biofilms on coverslips were rinsed thrice with PBS, followed then by labeling with 200 μl of the live/dead BacLight Bacterial Viability stain (L13152, Invitrogen, Carlsbad, CA, USA) and examined using an Olympus Fluoview FV10i confocal microscope

(Olympus, Tokyo, Japan). Live cells were stained with SYTO 9 (green fluorescence), and dead cells were stained with propidium iodide (PI; red fluorescence).

Scanning electron microscopy

To observe the morphological change of planktonic bacteria in the presence of **LN-7**, we used the scanning electron microscope (SEM, Merlin, Zeiss, Oberkochen, Germany). Briefly, exponential-phase cultures of *S. mutans* UA159 (~10^8 CFU/ml) were treated with or without **LN-7** at a final concentration of 2× MBC and incubated anaerobically for 24 h at 37 °C. Bacterial suspensions were centrifuged at 5000 *g* for 5 min, washed three times, and then resuspended in PBS. The subsequent procedures were performed as described previously [29].

Besides that, the effects of **LN-7** on the morphology change of preformed biofilms were also observed. 1-day old *S. mutans* biofilms were preformed in BHIS broth and treated with drugs as described in the study of treatment of preformed biofilms but instead in 6-well plates with coverslips in each well.

The biofilms were then treated with **LN-7**, CHX, or erythromycin at 10× their respective MICs in BHIS broth. The preparation of biofilm samples for SEM observation was as described for the planktonic samples above. The samples were then observed by SEM.

PI uptake assay

To detect the ability of the peptide to break the bacterial membrane, propidium iodide (PI) was used as a fluorescence probe for its ability to cross the disrupted membrane and stain the nucleic acids of cells [35]. Mid-logarithmic phase *S. mutans* UA159 was adjusted to 1×10^6 CFU/ml. The cells were, respectively, treated with or without **LN-7** dissolved in PBS at concentrations of 1× and 2× MBCs in centrifuge tubes. After 0, 5 and 10 min of incubation at 37 °C, the supernatants were removed and cells were washed twice with PBS. Then, 13.4 μM PI (Leagene, Beijing, China) was added to the cells and incubated for 30 min at room temperature. The cells were resuspended in 500 μl PBS after washing three times. The PI-positive cells were assessed by flow cytometry (FACSCanto II, BD, USA).

Circular dichroism (CD) spectroscopy

The CD spectra of the peptide solutions were recorded at room temperature using a CD spectrometer (ChirascanTM, Leatherhead, Surrey, UK) and a quartz cell with 0.5 cm path length. **LN-7** was dissolved to a final concentration of 250.0 μg/ml with PBS (pH 7.4, mimicking an aqueous environment), or supplemented with 50% (v/v) TFE (mimicking the hydrophobic environment of the microbial membrane) [36]. Spectra were recorded by scanning wavelength from 190 to 250 nm at 20 nm min^{-1}, and spectra averaged from four repeats. Spectra were analyzed using CDPro (http://lamar.colostate.edu/~sreeram/CDPro/main.html). Fractions of different types of secondary structure were calculated using three programs within the software (SELCON3, CONTINLL, and CDSSTR). The results of the three methods were averaged to give the final fractions.

In vivo animal study

To determine the effects of **LN-7** on the development of dental caries in vivo, a total of 24 rats were purchased from the Animal Lab Center of Southern Medical University (Guangzhou, China). Animal experiments were performed on a well-established rodent model of dental caries disease as described previously [37–39]. Briefly, 24 weaned Sprague–Dawley rats, 21 days old, were fed with ampicillin sodium water (4000 U/ml) and a regular diet for 3 days to lower the microbial load. Oral swabs were plated on Mitis salivarius agar (Solarbio, Beijing, China) and cultured anaerobically at 37 °C to confirm the absence of endogenous *S. mutans* infection. The animals were then offered cariogenic diet 2000# ad libitum throughout the experiment to enhance the infection by *S. mutans*. At 24 days old, the animals were infected orally using an actively growing (mid-logarithmic) culture of *S. mutans* UA159 every day for five consecutive days to allow oral colonization, and their infection was checked via oral swabbing. Then, the infected animals were randomly placed into treatment groups (8 animals/group), and their teeth were treated topically twice daily with saturated cotton swabs containing treatment solutions wiped on the molars during a uniform operating time of approximately 1 min. The treatment groups included: (1) 32 μM **LN-7** peptide solution, (2) 0.2% NaF (positive control), and (3) distilled deionized water (DDW; negative control).The experiment proceeded for 6 weeks; all animals were weighed weekly and their physical appearance was noted daily. At the end of the experimental period, the animals were sacrificed, and the jaws were surgically removed and aseptically dissected. All of the jaws were defleshed, molars of the animals were examined under a stereomicroscope and carious lesions were scored by the method of Keyes [40]. The determination of caries scores of the codified jaws was performed by a calibrated examiner.

Furthermore, the hemi-sectioned molars were prepared to be observed by the scanning electron microscope as described previously with a minor modification [41, 42]. First, the samples were fixed in 2.5% glutaraldehyde for 24 h and then washed in PBS to remove the fixative. After being dehydrated in increasing concentrations of ethanol, the samples were preserved at − 80 °C overnight and then

Table 1 Sequences and anti-*S. mutans* activities of **LN-7**, LR-1, known AMPs, and antimicrobial agents

Name	Sequence	*S. mutans* UA159	
		MIC (μM)	MBC (μM)
LN-7	LRWWLWKLLRRMR-NH2	3.3	6.5
LR-1	ATGTARKLLDAMA-NH2	> 151.8	> 151.8
LL-37	Ac-LLGDFFRKSKEKIGKEFKRIVQRIKDFLRN-LVPRTES-NH2	> 88.2	> 88.2
G2	KNLRIIRKGIHIIKKY-NH2	100.4	200.7
Pleurocidin	GWGSFFKKAAHVGKHVGKAALTHYL-NH2	4.6	9.2–18.4
CHX	$C_2H_{30}N_{10}C_{12}$·2HCL	2.0	8.0
Erythromycin	$C_{37}H_{67}NO_{13}$	0.04	1.4
Sodium fluoride	NaF	11,907.6 [0.05% (w/v)]	> 11,907.6

dried in a lyophilizer. The subsequent procedures for SEM were performed as described previously [29].

Statistical analysis

All experiments were performed in triplicate, and the data are presented as mean ± standard deviation. Statistical analysis was carried out using GraphPad Prism version 7.0 software (GraphPad Software, Inc., La Jolla, CA, USA) via a one-way analysis of variance (ANOVA) or Kruskal–Wallis *H* test. Statistical significance was defined as $P \leq 0.05$.

Results

Antimicrobial activity of LN-7

The cationic α-helical region of reutericin 6 and/or gassericin A was truncated and named LR-1. According to the principle of amphipathicity and cationicity of AMPs, we modified LR-1 into **LN-7**. To evaluate the antimicrobial potency of **LN-7** against *S. mutans* UA159, we made a comparison among **LN-7**, LR-1 and several peptide-based antimicrobial agents with established effects against *S. mutans* (Table 1). It was observed that compared with LR-1, **LN-7** exhibited obviously higher antimicrobial potency against *S. mutans* in the same condition with the MIC of 3.2 μM and MBC of 6.4 μM. In addition, the MICs of these known AMPs, except for LL-37, against *S. mutans* UA159 ranged from 4.6 to 100.4 μM, while **LN-7** exhibited higher antimicrobial potency against *S. mutans* UA159 under the same test condition.

Besides, the effectiveness of **LN-7** against other oral pathogenic bacteria was also tested. It turns out that **LN-7** was effective against *S. mutans, S. gordonii* and *S. sobrinus*, but showed relatively low antimicrobial effect on *E. faecalis*; MIC of 3.3 μM and MBC values ranged from 6.5 to 13.1 μM (Table 2).

Table 2 Susceptibility of other oral bacteria to **LN-7** in vitro

Species	Strain	MIC (μM)	MBC (μM)
Streptococcus mutans	ATCC25175	3.3	13.1
Streptococcus sobrinus	ATCC33478	3.3	6.5–13.1
Streptococcus gordonii	ATCC10558	3.3	6.5
Enterococcus faecalis	ATCC29212	> 104.6	> 104.6

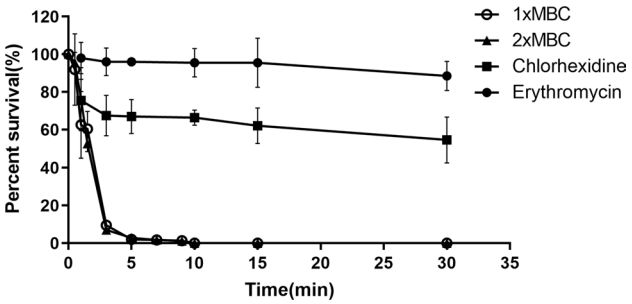

Fig. 1 Time-killing curves of **LN-7**. *S. mutans* UA159 was treated with **LN-7** (6.4 and 12.8 μM), CHX (19.8 μM) and erythromycin (2.7 μM). Results were presented with the percent survive and shown with mean ± standard deviation

Killing kinetics of LN-7

To assess the killing kinetics of **LN-7** against *S. mutans*, we performed a time-killing assay (Fig. 1). The results showed that **LN-7** was more efficient in killing *S. mutans* than CHX and erythromycin. More than 97% of the planktonic bacteria were killed within 5 min after treating with **LN-7**, and all *S. mutans* were killed in 10 min, whereas after treating with CHX or erythromycin for 30 min, survival percent of *S. mutans* still remained 54.6 and 88.5%, respectively. In addition, the antimicrobial activity of **LN-7** against planktonic *S. mutans* UA159 was dose- and time-dependent.

Next, we evaluated the killing kinetics of **LN-7** against single-species planktonic cultures of *S. mutans* UA159 and two closely related oral Streptococci, *S. sobrinus* ATCC33478 and *S. gordonii* ATCC10558. It was shown that within 15 min, nearly 95% of *S. gordonii* were killed and all *S. gordonii* were killed in 30 min. However, the killing rate against *S. sobrinus* is rather slower, with only 52% of *S. sobrinus* killed within 30 min (Fig. S1).

In addition, the killing kinetics was further assessed by measuring the absorbance value at 260 nm with ultraviolet spectrophotometer as indicated in Fig. S2. After a different treatment, the leakage of nucleic acid of dead bacteria was monitored. Melittin was used as the positive control for its known ability to disrupt bacterial membrane. We can see that **LN-7**, CHX and melittin exerted relatively fast killing rate. On the contrary, the killing kinetics of erythromycin is rather slower. Furthermore, the killing kinetics of **LN-7** against the other two types of Streptococci was consistent with the result of the colony-forming unit assay.

Effect of LN-7 on the formation and establishment of *S. mutans* biofilm

Given that the dental plaque formed by cariogenic bacterium is an important etiological factor for dental caries, we then tested the 50% minimum biofilm inhibitory concentration ($MBIC_{50}$) of **LN-7**, CHX, and erythromycin, which indicated the activity against the formation of *S. mutans* biofilm. The biofilm biomass was quantified after staining with crystal violet for 24 h and the results are presented in Fig. 2. The reduction of *S. mutans* biofilm formation jumped from 60.2% at 0.6× MIC to over 99.5% at 2× MIC of **LN-7**, indicating that the $MBIC_{50}$ of **LN-7** was 0.6× MIC, and LN-7 could nearly inhibit the formation of biofilm of *S. mutans* completely at the concentration of 2× MIC, as the same as CHX. However, erythromycin was less effective at inhibiting biofilm formation and required 4× MIC to achieve complete inhibition.

Next, we assessed the effect of **LN-7** on 1-d old *S. mutans* UA159 biofilm by quantifying the viable cells in the treated biofilm. We found that the ability of **LN-7**, CHX, and erythromycin to eradicate biofilms are dose-dependent (Fig. 3). At the concentration of 10 × MIC (32 μM), LN-7 could cause

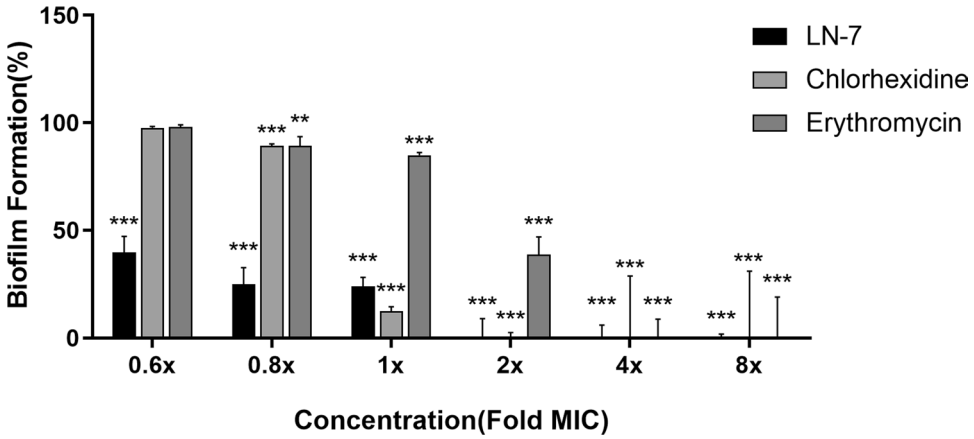

Fig. 2 Inhibitory effect of **LN-7** on formation of *S. mutans* biofilm. Biofilm formation assay was conducted in BHIS containing **LN-7**, CHX, and erythromycin at final concentrations of ×0.6, ×0.8×, ×1, ×2, ×4, ×8 their respective MICs for 24 h. Results were presented with the percentages of biofilm formation

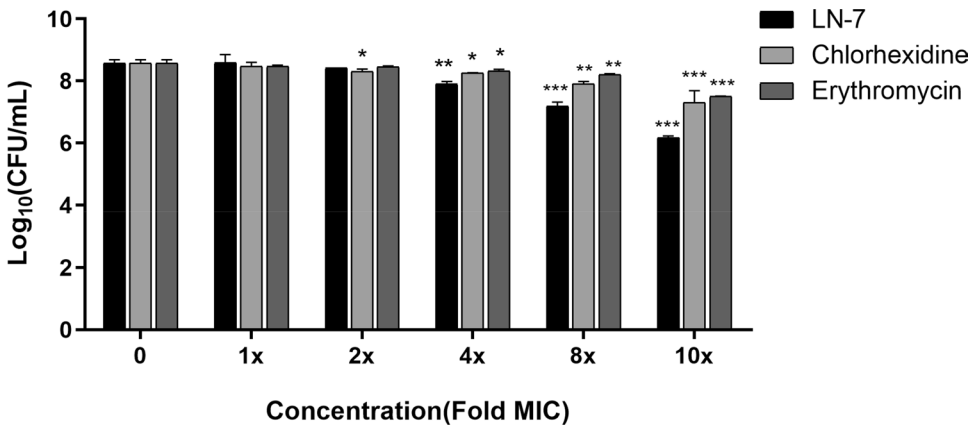

Fig. 3 Anti-biofilm activity of **LN-7** against preformed *S. mutans* biofilms. 1-d old biofilms of *S. mutans* UA159 were treated with **LN-7**, CHX and erythromycin at final concentrations of 1 to ×10 their respective MICs in BHIS for 24 h. Viable cells within biofilms were obtained by colony enumeration on agar plates

an overall 2.40-log10 reduction in the number of viable cells when compared with the untreated control. In contrast, CHX and erythromycin could only yielded a reduction in cell viability of 1.28- and 1.08-log10 at 10 × MIC, respectively.

Impairment of preformed biofilms visualized by confocal laser scanning microscopy (CLSM) and scanning electron microscopy (SEM)

After quantitative analysis, CLSM and SEM were used to reveal the changes of bacterial viability and morphology in the preformed biofilms treated with 10× MICs of **LN-7**. In the representative live/dead staining images (Figs. 4, 5), the green signal stands for vital bacteria with intact membranes, while the red signal stands for dead bacteria with destroyed membranes, and the yellow signal stands for the mixture. Biofilms incubated in the control group appeared dense and thick, with an average height of 21 μm, and no red signal was visualized. Conversely, the biofilm formed sparsely when added with **LN-7** and CHX. It was obvious that the images of **LN-7** showed thinner biofilms with an average height of 15 μm (Fig. 5) and more red signals when compared with the control group and erythromycin group (Fig. 4).

On the other hand, SEM depicted the impact of **LN-7** on the structural integrity of preformed biofilm (Fig. 6b). After exposure to **LN-7**, an essentially disrupted cellular network and porous exopolysaccharide matrix were observed and the cell aggregates were hard to form. Whereas, the control group as shown in Fig. 6a showed apparent clumping of cells with a formation of chains embedded into the exopolysaccharide pool. Also, only a little change was observed in CHX- and erythromycin-treated biofilms compared to untreated biofilms (Fig. 6c, d).

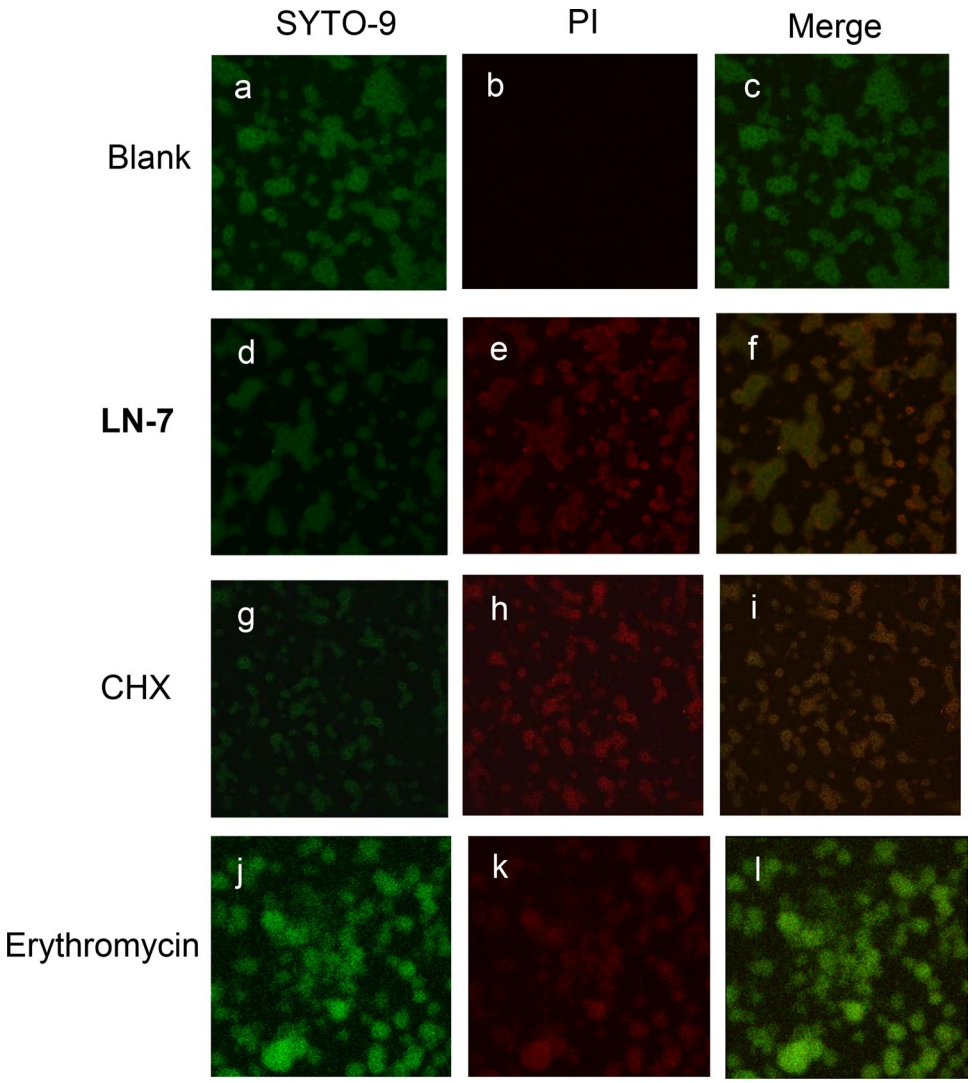

Fig. 4 Confocal fluorescent images of live, dead and merge bacterial cells in the absence (**a**–**c**) and the presence of **LN-7** (**d**–**f**), CHX (**g**–**i**) and erythromycin (**j**–**l**) at the concentration of ×10 MIC for 24 h

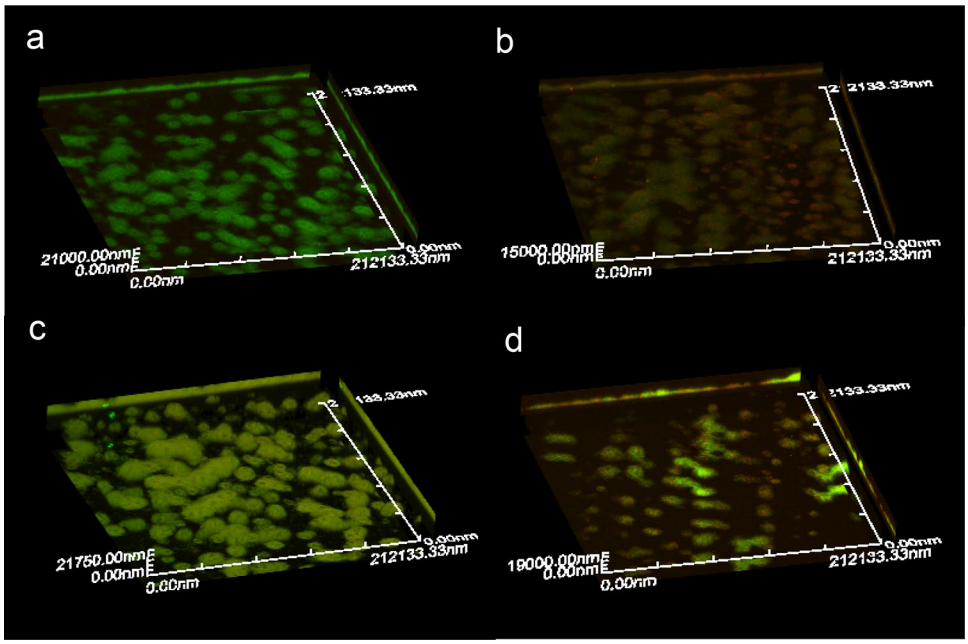

Fig. 5 The 3-dimensional reconstruction of *S. mutans* biofilms (live bacteria, stained green; dead cells, stained red) in the absence (**a**) and the presence of **LN-7** (**b**), erythromycin (**c**) and CHX (**d**)

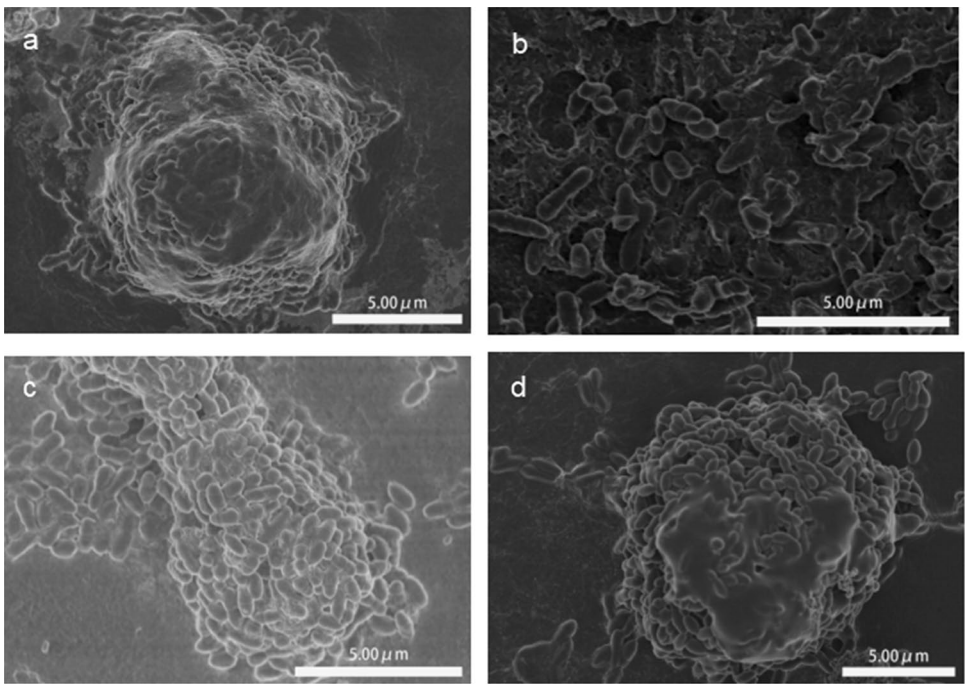

Fig. 6 SEM micrographs of preformed biofilms after 24 h treatment with BHI (**a**), **LN-7** (**b**), CHX (**c**) and erythromycin (**d**) at ×10 MIC

Mechanism of action of LN-7

It is acknowledged that disrupting membranes is one of the mechanisms of AMPs, which causes the lysis of microbial cells [43]. To explore the possible modes of action of **LN-7** using PI as a labeling reagent, we employed flow cytometry to investigate the interactions between **LN-7** and *S. mutans*. It was reported that PI is able to bind to double-stranded DNA by intercalating between base pairs, thus providing a rapid and reliable fluorescence method for monitoring dead bacterial cells injured by AMPs [33]. The observed red fluorescence stained by PI indicated that **LN-7** was able to break down the cell membrane, which, as a result, can lead to the leakage of nucleic acid labeled with the PI dye. With a 5 min exposure to **LN-7** at 12.8 μM, more than 96% of the *S. mutans* UA159 were stained with PI, which was in accordance with the result of the killing kinetics assays of **LN-7** against planktonic *S. mutans*, and the proportion of the PI-positive cells were dose- and time-dependent.

Also, SEM was used to observe morphology changes of *S. mutans* UA159 after treated with **LN-7**. As shown in Fig. 7a, in the absence of the peptide, *S. mutans* showed a regular, smooth surface. When exposed to 2× MBC of **LN-7**, *S. mutans* obviously altered bacterial morphology: cells lost their original form (Fig. 7b), small holes and ruptures of membrane visible (Fig. 7c), and aggregates of cellular debris (Fig. 7d).

Secondary structure of LN-7

The secondary structures of **LN-7** in water or 50% (v/v) TFE/water, which mimicked a hydrophobic membrane environment, were assessed using CD spectroscopy. As shown in Fig. 8, the CD spectrum of **LN-7** in PBS and 50% TFE/water both exhibited two negative minimum peaks at 208 and 222 nm, indicating that the peptides adopted a well-defined α-helical structure. The calculated percentage of secondary structure elements for **LN-7** was 98.85% α-helix and 5.98% β-turn in PBS, 99.60% α-helix and 5.30% β-turn in 50% TFE/water solution.

Prevention of dental caries in vivo

To assess whether **LN-7** would exert effects in the complex oral environment in vivo, we then carried out an in vivo animal study. The experimental design and treatment regimen are illustrated in Fig. 9. It was observed that body weight was similar across all rats in three groups throughout the experiment, as shown in Fig. 10, and the rats remained apparently healthy and active. Moreover, no macroscopic tissue lesions or abnormalities were observed on the mucosa of the animals during the whole experiment, which proved the relative safeness of **LN-7**.

The carious lesions established on the occlusal surface were scored according to the penetration depth of murexide as enamel caries (*E*), slight dentinal caries (D_s), moderate dentinal caries (D_m) or external dentinal caries (D_x) [42], while lesions detected on smooth surface influenced only on enamel layer. All the scores were depicted in Table 3. In addition, representative images of carious lesions of three groups were obtained as shown in Fig. 11. Quantitative caries scoring analyses revealed that compared with the negative control, the **LN-7** group presented significantly less overall carious lesions ($P < 0.05$). Also, **LN-7** was highly effective in decreasing enamel and slight dentinal lesions in sulcal surfaces, similar to the effect of 0.2% NaF treatment ($P > 0.05$).

Moreover, we observed the characterization of the fissure caries with the scanning electronic microscope (Fig. 12). The murexide-negative fissures on the molar showed no cavitation on enamel. The uniform contrast of dentin underneath indicated no significant demineralization activity. The murexide-positive lesion located on the fissures on the molar, however, exhibited fissure caries with a different degree of severity. According to Fig. 12, we can see that the surface of the fissure on the molar in 0.2% NaF group was smooth and continuous (Fig. 12a), and we can clearly tell the enamel-dentinal junction as indicated by the hollow arrow. As for the **LN-7** group (Fig. 12b), slight erosion on the enamel was observed, indicated by the solid arrow; however, the enamel-dentinal junction and dentin were intact.

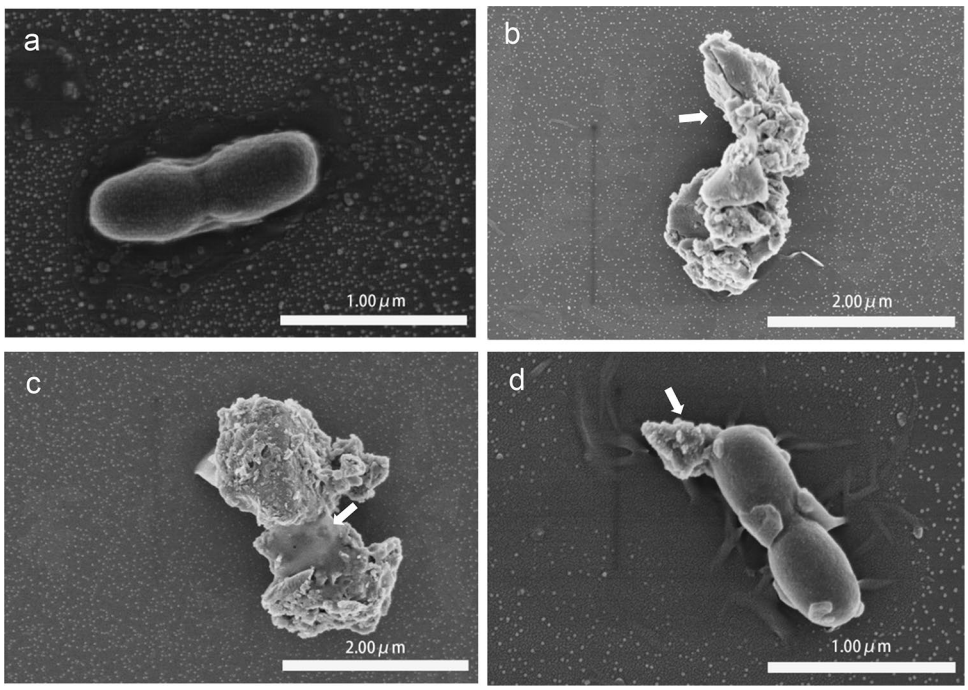

Fig. 7 Membrane damage caused by **LN-7**. *S. mutans* UA159 (1×10^8 CFU/ml) after exposed to **LN-7** at 12.8 μM for 1 h are compared with untreated cells (**a**). White arrows indicate collapsed cells (**b**), pore formation (**c**) and aggregates of cellular debris (**d**)

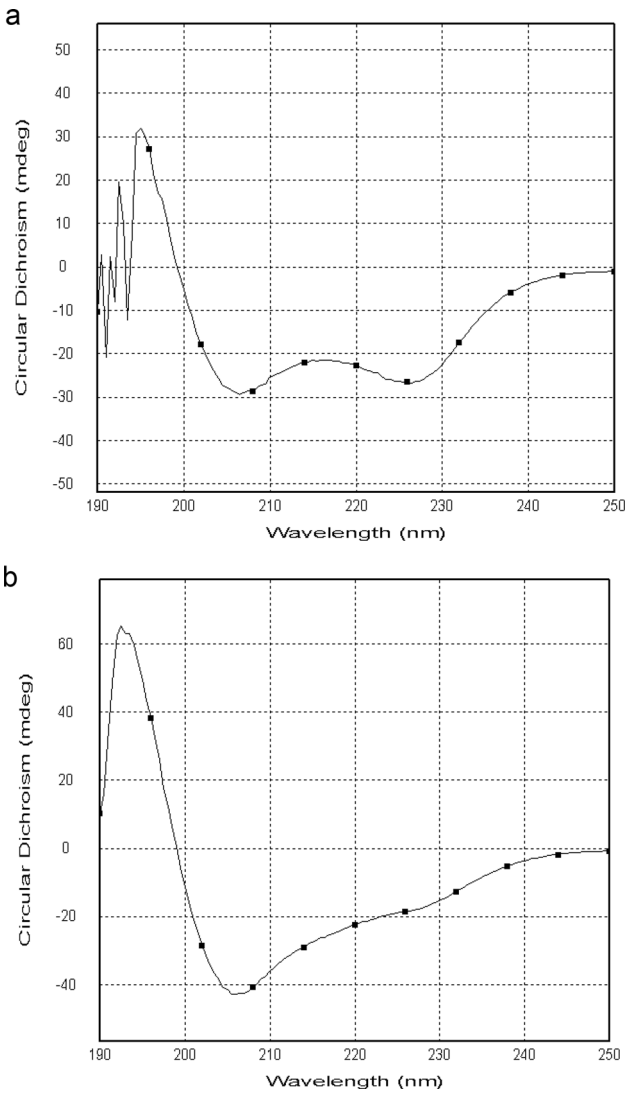

Fig. 8 Circular dichroism (CD) spectrum of **LN-7** in PBS (**a**) or 50% trifluoroethanol (TFE)/water (**b**)

The defect was about 13 μm in depth. On the other hand, the surface of the fissure on the molar in DDW group was damaged heavily, which showed a cavitation about 65 μm in depth and had destroyed the enamel-dentinal junction (Fig. 12c).

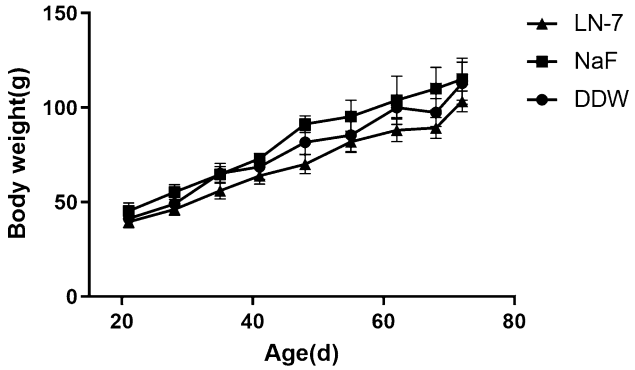

Fig. 10 Body weight changes of Sprague–Dawley rats in different treatment groups throughout the experiment

Discussion

It is known that AMPs with cationicity can initially interact with cells through the attraction to the anionic electrostatic charge of biological membranes. In addition, amphipathicity is a prerequisite for α-helical AMP activity, which enables AMPs to bind to anionic phospholipid head groups of the exterior leaflet of bacterial membranes through electrostatic attraction and, thus, exhibit permeabilizing and/or disrupting activity [44, 45]. In our study, we first truncated the cationic α-helical region of reutericin 6 or gassericin A, named as LR-1, and then exploited existing design strategies [46] to modify it into a novel short linear peptide, **LN-7**. After the modification, the peptide showed perfect amphipathic arrangement and cationicity, which laid a foundation for the following experimental results that showed that compared with LR-1, **LN-7** was more effective against *S. mutans*. Furthermore, confirmed by CDPro analysis, the secondary structure of **LN-7** characterized by CD spectroscopy suggested that **LN-7** adopted a helical structure in membrane-mimetic solvents (50% TFE), with a proportion of α- helical structure of 99.6%. The secondary structure of **LN-7** characterized by CD spectroscopy suggested that **LN-7** adopted a helical structure in membrane-mimetic solvents (50% TFE). It was proposed that percent helical composition >80% was correlated with antimicrobial potency [47]. The high percent

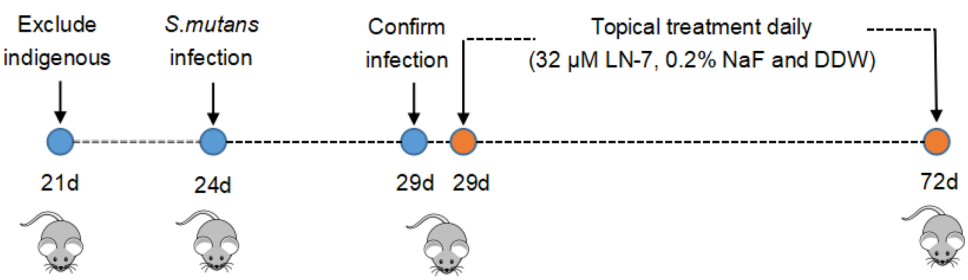

Fig. 9 Experimental design and treatment regimen of the in vivo animal study

Table 3 Evaluation of Keyes caries scoring method on occlusal and smooth surfaces of molars in rats compared across experimental groups

Treatment	Occlusal surface				Smooth surface
	E	D_s	D_m	D_x	*E*
DDW	16.4 ± 3.8^{a}	10.4 ± 4.9^{c}	3.7 ± 3.2^{e}	0.6 ± 0.9^{f}	19.3 ± 2.7^{g}
NaF	8.7 ± 4.3^{b}	$7.2 \pm 4.5^{c,d}$	2.5 ± 1.7^{e}	0.2 ± 0.4^{f}	11.5 ± 3.8^{h}
LN-7	6.6 ± 1.9^{b}	5.3 ± 2.0^{d}	1.9 ± 2.3^{e}	0^{f}	9.7 ± 7.4^{h}

[a-h]Values labeled with different superscript letters in the same column denote significant statistical difference among treatments (One-way ANOVA, $P \leq 0.05$)

helical composition of **LN-7** suggested its well antimicrobial potency.

It is usually recommended that the duration of rinsing mouth and tooth brushing is about 3–5 min. Compared with the commonly used antimicrobial agents, chlorhexidine and erythromycin, **LN-7** showed faster killing kinetics against planktonic *S. mutans*, which caused about 97% reduction in viability of *S. mutans* within 5 min at 12.5 μM, indicating its potential to be used in mouth rinses or toothpaste, assuming that its antimicrobial activity and stability in human saliva can be confirmed. In addition, given its shown effects against other types of Streptococci in the study, **LN-7** may be a novel antimicrobial agent with relatively broad spectrum. Interestingly, our data have shown that the killing kinetics of **LN-7** against *S. mutans* is about much faster than that against *S. sorbrinus* and *S. gordonii* in 5 min, which suggested that **LN-7** may possess a selectively antimicrobial capability targeting *S. mutans* within a short time. It was demonstrated that selectively targeting of *S. mutans* biofilms is feasible and can effectively prevent dental caries without disturbing the overall oral microbiome [48], appealing further modification of **LN-7**. For example, combining **LN-7** with the competence-stimulating peptide (CSP) [49], which is able to target *S. mutans*, may conduce to the selectivity of **LN-7**, but it requires further study.

Literatures have reported that biofilm-associated microorganisms behaved differently from their planktonic counterparts on their ability to resist drug treatment and host defenses [50]. A unique, highly protected phenotypic state adopted by the microorganisms in a biofilm, called persister cells, which were first identified by Joseph Bigger in 1944, contribute to the difference [51]. The persister cells are dormant and have little translation or topoisomerase activity,

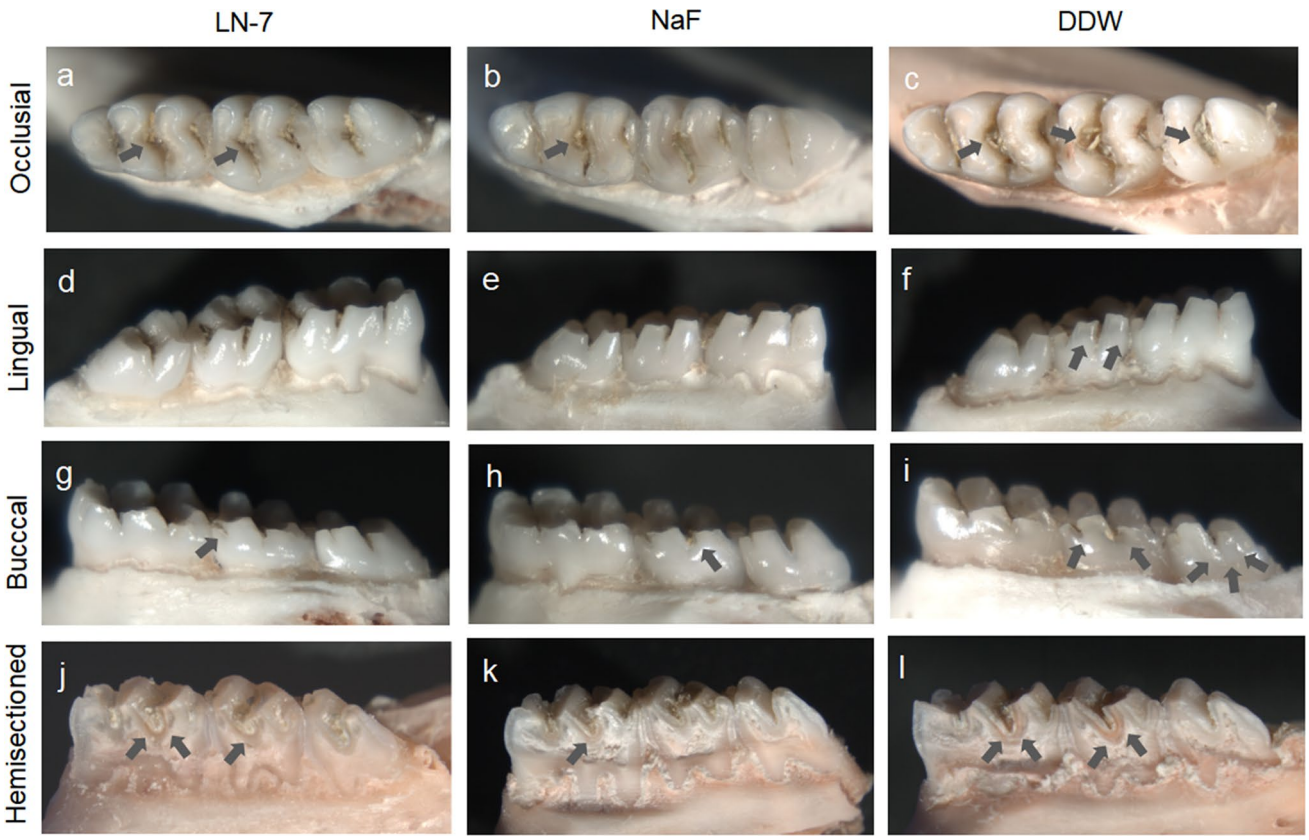

Fig. 11 Representative images of molars of Sprague–Dawley rats after treatment of distilled and deionized water (DDW), 0.2% NaF, and 32 μM **LN-7,** respectively. In each group, images of occlusal surface (**a**–**c**), lingual surface (**d**–**f**), buccal surface (**g**–**i**) and hemisectioned teeth (**j**–**l**) were photographed. Arrows indicate the carious lesions

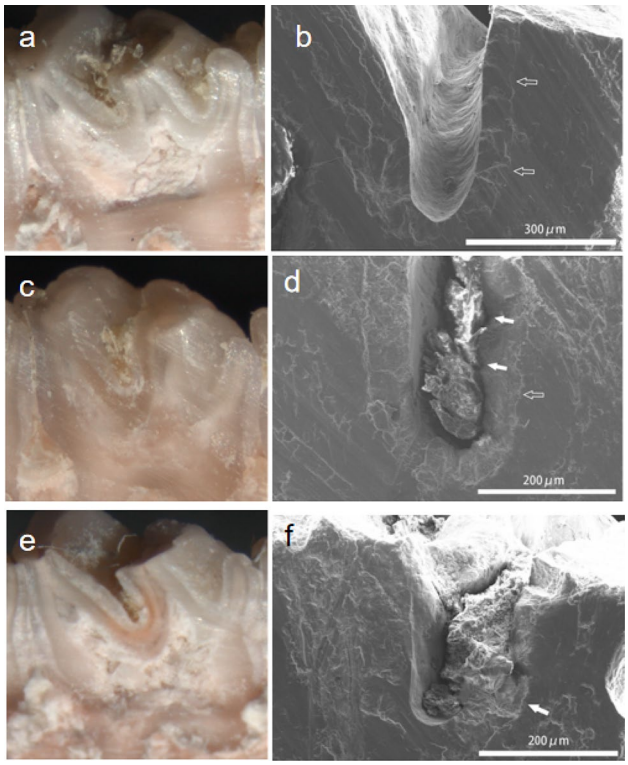

Fig. 12 Stereomicroscopy and SEM images of the hemi-sectioned molar teeth in NaF group (**a**, **b**), LN-7 group (**c**, **d**), and DDW group (**e**, **f**). Hollow arrows indicate the enamel dentin junction, and solid arrows indicate the caries lesions

which enables resistance to killing by antibiotics. Reduced antimicrobial efficacy in biofilm-related disease results from the fact that almost all conventional antibiotics target the biosynthetic processes taking place in actively growing bacteria, including the biosynthesis of proteins, RNA, DNA, peptidoglycan and folic acid [52]. Therefore, conventional antibiotics show little efficacy in killing non-multiplying bacteria, in other words, persisters [53], and this is consistent with the result of our biofilm susceptibility assays, which showed that erythromycin exerted little inhibition of biofilm formation and preformed biofilm. However, biofilm susceptibility assays indicated that **LN-7** could effectively inhibit the preformed biofilm of *S. mutans* at 10-fold MIC, and we further applied this concentration of **LN-7** in the subsequent studies relevant to biofilm, including observation of the impairment of biofilm with CLSM and SEM, as well as the in vivo animal study [37, 54]. Results of the CLSM observation showed that compared with those in the control group and erythromycin group, the *S. mutans* biofilm in the **LN-7** group appeared thinner and sparser, with more red signals in images, which indicated the effective antibacterial potency of **LN-7**, in agreement with those results of colony-forming count method. Furthermore, SEM images illustrated that biofilm treated with **LN-7** was incompact and sparse, suggesting that combined with the use of mechanical cleaning, **LN-7** may effectively eradicate biofilms.

The efficacy of **LN-7** in inhibiting biofilm of *S. mutans* may be due to the mechanism of its antimicrobial activity. It was reported that AMPs function mainly based on the action on the bacterial membrane, which is different from the antimicrobial mechanism of conventional antibiotics [44], and may contribute to its rapid killing kinetics and less resistance selection, while other mechanisms of AMPs were also reported, such as intracellular targeting and activation of host cells immunomodulation [55]. We then preliminary explored the antibacterial mechanism of **LN-7** and found that it was able to disrupt the membrane of bacteria, which was consistent with most peptides, especially those with fast killing kinetics [56]. However, further studies about the mechanism of the inhibition against the biofilm of *S. mutans* are needed, for example, the effect of **LN-7** on extracellular polymeric substance, the matrix of biofilm.

To further assess the anti-caries effect of **LN-7** in the complex oral environment, we used a well-established rodent model of dental caries [37–39]. Our findings corroborated that the **LN-7** group performed significantly less enamel and slight dentinal lesions in the sulcal surface compared with the DDW group. Moreover, **LN-7** groups also showed significantly less smooth surface lesions compared with the DDW group, even reaching the extent to NaF, which is considered as the gold standard in the prevention of caries [57]. In addition, it was reported that the accuracy of overall caries scores of rats can be enhanced by SEM images [42], and our results showed that SEM images could provide more detailed structure of the molars and exhibit the caries progression more clearly. The results of the animal study suggested that **LN-7** may help to thwart the progression of dental caries in vivo. Notably, throughout the experiment, there were no signs of deleterious effects on the rats' body weight or to the mucosa, suggesting the low local toxicity of **LN-7**. Nevertheless, full toxicity studies should be conducted to determine the long-term effects of daily topical applications of **LN-7**.

Dental caries is a multifactorial disease, whose progression is determined by a variety of factors, including the susceptible host, cariogenic microorganism, diet, and time. The key elements of anti-caries biological approaches lie in the use of remineralizing agents to the tooth structure and the regulation of cariogenic biofilms [58]. Our data supported that **LN-7** exhibits certain capability of preventing dental caries, which may result from the anti-biofilm ability of **LN-7** against *S. mutans*. However, the underlying mechanism requires further exploration.

In conclusion, this study clearly demonstrated the ability of a derivative of reutericin 6 and gassericin A to inhibit the biofilm of *S. mutans* UA159 and prevent dental

caries in a rat model, justifying further studies under a broader range of cariogenic conditions, and the knowledge obtained in the study may provide a basis for the development of a feasible new anti-biofilm and anti-caries alternative product for therapeutic use.

Acknowledgements The work was supported by the Science and Technology Department of Guangdong Province of China (2018B030311047) and the Science and Technology Program of Guangzhou, China (201804010419).

Compliance with ethical standards

Conflict of interest The authors declare that they have no conflict of interest.

References

1. Takahashi N, Nyvad B. The role of bacteria in the caries process: ecological perspectives[J]. J Dent Res. 2011;90(3):294–303.
2. Bernardi S, Continenza MA, Al-Ahmad A, et al. *Streptococcus* spp. and *Fusobacterium nucleatum* in tongue dorsum biofilm from halitosis patients: a fluorescence in situ hybridization (FISH) and confocal laser scanning microscopy (CLSM) study[J]. New Microbiol. 2019;42(2):108–13.
3. Bernardi S, Karygianni L, Filippi A, et al. Combining culture and culture-independent methods reveals new microbial composition of halitosis patients' tongue biofilm[J]. Microbiologyopen. 2020;9(2):e958.
4. Bernardi S, Bianchi S, Botticelli G, et al. Scanning electron microscopy and microbiological approaches for the evaluation of salivary microorganisms behaviour on anatase titanium surfaces: in vitro study[J]. Morphologie. 2018;102(336):1–6.
5. Bernardi S, Bianchi S, Tomei AR, et al. Microbiological and SEM-EDS evaluation of titanium surfaces exposed to periodontal gel: in vitro study[J]. Materials. 2019;12(9):1448.
6. Patianna G, Valente NA, D'Addona A, et al. In vitro evaluation of controlled-release 14% doxycycline gel for decontamination of machined and sandblasted acid-etched implants[J]. J Periodontol. 2018;89(3):325–30.
7. Meza-Siccha AS, Aguilar-Luis MA, Silva-Caso W, et al. In vitro evaluation of bacterial adhesion and bacterial viability of *Streptococcus mutans*, *Streptococcus sanguinis*, and *Porphyromonas gingivalis* on the abutment surface of titanium and zirconium dental implants[J]. Int J Dent. 2019;2019:4292976.
8. Zijnge V, van Leeuwen MB, Degener JE, et al. Oral biofilm architecture on natural teeth[J]. PLoS One. 2010;5(2):e9321.
9. Kawada-Matsuo M, Komatsuzawa H. Role of *Streptococcus mutans* two-component systems in antimicrobial peptide resistance in the oral cavity[J]. Jpn Dent Sci Rev. 2017;53(3):86–94.
10. Min KR, Galvis A, Williams B, et al. Antibacterial and antibiofilm activities of a novel synthetic cyclic lipopeptide against cariogenic *Streptococcus mutans* UA159[J]. Antimicrob Agents Chemother. 2017;61(8):e00776-17.
11. Jiang W, Wang Y, Luo J, et al. Effects of antimicrobial peptide GH12 on the cariogenic properties and composition of a cariogenic multispecies biofilm[J]. Appl Environ Microbiol. 2018;84(24):e01423-18.
12. Guo L, McLean JS, Yang Y, et al. Precision-guided antimicrobial peptide as a targeted modulator of human microbial ecology[J]. Proc Natl Acad Sci USA. 2015;112(24):7569–74.
13. Zanatta FB, Antoniazzi RP, Rosing CK. Staining and calculus formation after 0.12% chlorhexidine rinses in plaque-free and plaque covered surfaces: a randomized trial[J]. J Appl Oral Sci. 2010;18(5):515–21.
14. McCormick TS, Weinberg A. Epithelial cell-derived antimicrobial peptides are multifunctional agents that bridge innate and adaptive immunity[J]. Periodontol 2000. 2010;54(1):195–206.
15. Guaní-Guerra E, Santos-Mendoza T, Lugo-Reyes SO, et al. Antimicrobial peptides: general overview and clinical implications in human health and disease[J]. Clin Immunol. 2010;135(1):1–11.
16. Sierra JM, Fuste E, Rabanal F, et al. An overview of antimicrobial peptides and the latest advances in their development[J]. Expert Opin Biol Ther. 2017;17(6):663–76.
17. Helmerhorst EJ, Hodgson R, Van't Hof W, et al. The effects of histatin-derived basic antimicrobial peptides on oral biofilms[J]. J Dent Res. 1999;78(6):1245–50.
18. Kreling PF, Aida KL, Massunari L, et al. Cytotoxicity and the effect of cationic peptide fragments against cariogenic bacteria under planktonic and biofilm conditions[J]. Biofouling. 2016;32(9):995–1006.
19. Tao R, Tong Z, Lin Y, et al. Antimicrobial and antibiofilm activity of pleurocidin against cariogenic microorganisms[J]. Peptides. 2011;32(8):1748–54.
20. Wang W, Tao R, Tong Z, et al. Effect of a novel antimicrobial peptide chrysophsin-1 on oral pathogens and *Streptococcus mutans* biofilms[J]. Peptides. 2012;33(2):212–9.
21. Maisetta G, Batoni G, Esin S, et al. Susceptibility of *Streptococcus mutans* and *Actinobacillus actinomycetemcomitans* to bactericidal activity of human beta-defensin 3 in biological fluids[J]. Antimicrob Agents Chemother. 2005;49(3):1245–8.
22. Ding Y, Wang W, Fan M, et al. Antimicrobial and anti-biofilm effect of Bac8c on major bacteria associated with dental caries and *Streptococcus mutans* biofilms[J]. Peptides. 2014;52:61–7.
23. Kang MS, Oh JS, Lee HC, et al. Inhibitory effect of *Lactobacillus reuteri* on periodontopathic and cariogenic bacteria[J]. J Microbiol. 2011;49(2):193–9.
24. Koll-Klais P, Mandar R, Leibur E, et al. Oral lactobacilli in chronic periodontitis and periodontal health: species composition and antimicrobial activity[J]. Oral Microbiol Immunol. 2005;20(6):354–61.
25. Soderling EM, Marttinen AM, Haukioja AL. Probiotic lactobacilli interfere with *Streptococcus mutans* biofilm formation in vitro[J]. Curr Microbiol. 2011;62(2):618–22.
26. Kawai Y, Ishii Y, Arakawa K, et al. Structural and functional differences in two cyclic bacteriocins with the same sequences produced by lactobacilli[J]. Appl Environ Microbiol. 2004;70(5):2906–11.
27. Torcato IM, Huang YH, Franquelim HG, et al. Design and characterization of novel antimicrobial peptides, R-BP100 and RW-BP100, with activity against Gram-negative and Gram-positive bacteria[J]. Biochim Biophys Acta. 2013;1828(3):944–55.
28. Won HS, Park SH, Kim HE, et al. Effects of a tryptophanyl substitution on the structure and antimicrobial activity of C-terminally truncated gaegurin 4[J]. Eur J Biochem. 2002;269(17):4367–74.
29. Zhu X, Zhang L, Wang J, et al. Characterization of antimicrobial activity and mechanisms of low amphipathic peptides with different alpha-helical propensity[J]. Acta Biomater. 2015;18:155–67.
30. Fang Y, Zhong W, Wang Y, et al. Tuning the antimicrobial pharmacophore to enable discovery of short lipopeptides with multiple modes of action[J]. Eur J Med Chem. 2014;83:36–44.

31. Eckert R, Qi F, Yarbrough DK, et al. Adding selectivity to antimicrobial peptides: rational design of a multidomain peptide against *Pseudomonas* spp[J]. Antimicrob Agents Chemother. 2006;50(4):1480–8.
32. Limsuwan S, Moosigapong K, Jarukitsakul S, et al. Lupinifolin from *Albizia myriophylla* wood: a study on its antibacterial mechanisms against cariogenic *Streptococcus mutans*[J]. Arch Oral Biol. 2018;93:195–202.
33. Chen Z, Yang G, Lu S, et al. Design and antimicrobial activities of LL-37 derivatives inhibiting the formation of *Streptococcus mutans* biofilm[J]. Chem Biol Drug Des. 2019;93(6):1175–85.
34. O'Toole GA, Kolter R. Initiation of biofilm formation in *Pseudomonas fluorescens* WCS365 proceeds via multiple, convergent signalling pathways: a genetic analysis[J]. Mol Microbiol. 1998;28(3):449–61.
35. Chatterjee A, Perevedentseva E, Jani M, et al. Antibacterial effect of ultrafine nanodiamond against Gram-negative bacteria *Escherichia coli*[J]. J Biomed Opt. 2015;20(5):51014.
36. Tu H, Fan Y, Lv X, et al. Activity of synthetic antimicrobial peptide GH12 against oral Streptococci[J]. Caries Res. 2016;50(1):48–61.
37. Kim D, Liu Y, Benhamou RI, et al. Bacterial-derived exopolysaccharides enhance antifungal drug tolerance in a cross-kingdom oral biofilm[J]. ISME J. 2018;12(6):1427–42.
38. Naha PC, Liu Y, Hwang G, et al. Dextran-coated iron oxide nanoparticles as biomimetic catalysts for localized and pH-activated biofilm disruption[J]. ACS Nano. 2019;13(5):4960–71.
39. Bowen WH. Rodent model in caries research[J]. Odontology. 2013;101(1):9–14.
40. Keyes PH. Dental caries in the molar teeth of rats. II. A method for diagnosing and scoring several types of lesions simultaneously[J]. J Dent Res. 1958;37(6):1088–99.
41. Naylor F, Aranha ACC, Eduardo CDP, et al. Micromorphological analysis of dentinal structure after irradiation with Nd:YAG laser and immersion in acidic beverages[J]. Photomed Laser Surg. 2006;24(6):745.
42. Yucesoy DT, Fong H, Gresswell C, et al. Early caries in an in vivo model: structural and nanomechanical characterization[J]. J Dent Res. 2018;97(13):1452–9.
43. Brogden KA. Antimicrobial peptides: pore formers or metabolic inhibitors in bacteria?[J]. Nat Rev Microbiol. 2005;3(3):238–50.
44. Takahashi D, Shukla SK, Prakash O, et al. Structural determinants of host defense peptides for antimicrobial activity and target cell selectivity[J]. Biochimie. 2010;92(9):1236–41.
45. Wiradharma N, Sng MY, Khan M, et al. Rationally designed alpha-helical broad-spectrum antimicrobial peptides with idealized facial amphiphilicity[J]. Macromol Rapid Commun. 2013;34(1):74–80.
46. Liang D, Li H, Xu X, et al. Rational design of peptides with enhanced antimicrobial and anti-biofilm activities against cariogenic bacterium *Streptococcus mutans*[J]. Chem Biol Drug Des. 2019;94:1768–81.
47. Deslouches B, Phadke SM, Lazarevic V, et al. De novo generation of cationic antimicrobial peptides: influence of length and tryptophan substitution on antimicrobial activity[J]. Antimicrob Agents Chemother. 2005;49(1):316–22.
48. Garcia SS, Blackledge MS, Michalek S, et al. Targeting of *Streptococcus mutans* biofilms by a novel small molecule prevents dental caries and preserves the oral microbiome[J]. J Dent Res. 2017;96(7):807–14.
49. Kaplan CW, Sim JH, Shah KR, et al. Selective membrane disruption: mode of action of C16G2, a specifically targeted antimicrobial peptide[J]. Antimicrob Agents Chemother. 2011;55(7):3446–52.
50. Fux CA, Costerton JW, Stewart PS, et al. Survival strategies of infectious biofilms[J]. Trends Microbiol. 2005;13(1):34–40.
51. Del PJ. Biofilm-related disease[J]. Expert Rev Anti Infect Ther. 2018;16(1):51–65.
52. Hurdle JG, O'Neill AJ, Chopra I, et al. Targeting bacterial membrane function: an underexploited mechanism for treating persistent infections[J]. Nat Rev Microbiol. 2011;9(1):62–75.
53. Coates AR, Hu Y. Targeting non-multiplying organisms as a way to develop novel antimicrobials[J]. Trends Pharmacol Sci. 2008;29(3):143–50.
54. Bueno-Silva B, Koo H, Falsetta ML, et al. Effect of neovestitol-vestitol containing Brazilian red propolis on accumulation of biofilm in vitro and development of dental caries in vivo[J]. Biofouling. 2013;29(10):1233–42.
55. Mai S, Mauger MT, Niu L, et al. Potential applications of antimicrobial peptides and their mimics in combating caries and pulpal infections[J]. Acta Biomater. 2017;49:16–35.
56. de Breij A, Riool M, Cordfunke RA, et al. The antimicrobial peptide SAAP-148 combats drug-resistant bacteria and biofilms[J]. Sci Transl Med. 2018;10(423):eaan4044.
57. Clarkson JJ, McLoughlin J. Role of fluoride in oral health promotion[J]. Int Dent J. 2000;50(3):119–28.
58. Baptista A, Kato IT, Prates RA, et al. Antimicrobial photodynamic therapy as a strategy to arrest enamel demineralization: a short-term study on incipient caries in a rat model[J]. Photochem Photobiol. 2012;88(3):584–9.